

The Activation of NLRP3 Inflammasome Potentiates the Immunomodulatory Abilities of Mesenchymal Stem Cells in Murine Colitis Model

Ji-Su Ahn

Pusan National University

Yoojin Seo

Pusan National University

Su-Jeong Oh

Pusan National University

Ji Won Yang

Pusan National University

Ye Young Shin

Pusan National University

Byung-Chul Lee

Seoul National University

Kyung-Sun Kang

Seoul National University

Eui-Suk Sung

Pusan National University Yangsan Hospital

Byung-Joo Lee

Pusan National University Yangsan Hospital

Tae-Hoon Shin

National Institutes of Health

Hyung-Sik Kim (✉ hskimcell@pusan.ac.kr)

Pusan National University School of Dentistry

Research

Keywords: mesenchymal stem cell, inflammasome, NLRP3, immunomodulation, colitis

Posted Date: February 18th, 2020

DOI: <https://doi.org/10.21203/rs.2.23882/v1>

License: © ⓘ This work is licensed under a Creative Commons Attribution 4.0 International License.

[Read Full License](#)

Abstract

Background

Inflammasomes are cytosolic, multiprotein complexes which act at the frontline of the immune responses by recognizing pathogen or danger-associated molecular patterns of pathogens or abnormal host molecules. Mesenchymal stem cells (MSCs) have been reported to possess multipotency to differentiate into various cell types and immunoregulatory effects which make them a promising treatment for regenerative medicine and immune-related diseases, respectively. However, little is known about the expression and role of the inflammasome in adult stem cells. In this study, we investigated the expression and functional regulation of NLRP3 inflammasome in human umbilical cord blood-derived MSCs (hUCB-MSCs).

Methods

The expression of NLR Family Pyrin Domain Containing 3 (NLRP3) inflammasome was detected in hUCB-MSCs. Cell proliferation, death and differentiation were analyzed after NLRP3 inflammasome activation. To investigate the changes in immunoregulatory functions of hUCB-MSCs, naïve or NLRP3 inflammasome-stimulated cells were infused into chemically induced colitic mice and symptoms were monitored.

Results

NLRP3 inflammasome activation suppressed the differentiation of hUCB-MSCs into osteoblasts, which was restored when the expression of adaptor proteins for inflammasome assembly was inhibited. Moreover, the suppressive effects of MSCs on T cell responses and the macrophage activation were augmented in response to NLRP3 activation. In vivo studies using colitic mice revealed that the protective abilities of hUCB-MSCs increased after NLRP3 stimulation.

Conclusions

Our findings suggest that the NLRP3 inflammasome components are expressed in hUCB-MSCs and its activation can regulate the differentiation capability and the immunomodulatory effects of hUCB-MSCs.

Introduction

The mammalian immune system consists of innate and adaptive immunity, which cooperatively work for the elimination of exogenous pathogens or endogenous danger signals. The innate immune system eradicates the infective microbial pathogens upon their recognition and initiates further inflammatory responses (1–4). The innate immune cells possess various sensor proteins to distinguish self-molecules from foreign substances (5, 6). Pattern recognition receptors (PRRs) are sensors for pathogen-associated molecular patterns (PAMPs), including lipopolysaccharides (LPS), lipoteichoic acid, peptidoglycan (PGN), lipopeptides and microbial nucleic acids (7). Toll-like receptors (TLRs) and Nod-like receptors (NLRs) are

representative families of PRRs. Agonists for both receptor families have been reported to trigger the NF- κ B and mitogen-activated protein kinase (MAPK) in immune cells, followed by the cytokine production (8–10). Previous studies have reported that TLRs and NLRs are functionally expressed in MSCs (11–15). In our previous study, the stimulation of nucleotide-binding oligomerization domain 2 (NOD2) resulted in the altered differentiation capabilities or immunoregulatory abilities (14). Inflammasome is the recently reported cytosolic protein complex which is involved in the initiation of the inflammatory responses in response to exogenous microbial infection and endogenous danger signals. Inflammasome generally contains three components: a cytosolic PRR (NLR or AIM2-like receptor family) that senses stimuli, the enzyme caspase-1 which converts cytokine precursors into mature cytokines, and apoptosis-associated speck-like protein containing a caspase recruitment domain (ASC), the adaptor protein (16, 17). Assembly of the inflammasome leads to the activation of caspase-1 which subsequently transforms the pro-inflammatory cytokines such as interleukin-1 β (IL-1 β) and interleukin-18 (IL-18) to their mature and active forms (18).

The NLRP3 inflammasome has been well studied and most frequently implicated as a key player in the pathogenesis of various diseases. Unlike to inflammasomes containing other NLR family members as the sensor, the basal expression of NLRP3 is not enough for activation. NLRP3 inflammasome is activated via two-step processes including priming step (first step) and activation step (second step) (19, 20). Currently, little is known about the expression and role of inflammasome in non-immune cells including adult stem cells.

Mesenchymal stem cells (MSCs) have been reported to exhibit immunoregulatory properties against a number of immune disorders including multiple sclerosis, sepsis, inflammatory bowel disease, rheumatoid arthritis, type I diabetes and graft-versus-host-disease, as well as differentiation potential into mesodermal lineages (21–26). This immunomodulatory ability of MSCs on immune cells is mostly exerted by soluble factors such as prostaglandin-E2 (PGE₂), nitric oxide (NO), indoleamine 2,3-dioxygenase-1 (IDO-1), transforming growth factor (TGF- β 1) and galectins (27–33). In our previous findings, we showed that the priming of NOD2 receptors in mesenchymal stem cells before the administration led to the improved therapeutic efficacy against colitis and atopic dermatitis by regulating T cells or mast cells, respectively, via the production of PGE₂ [34, 35]. Although few studies including the one by Oh et al. revealed that MSCs can regulate the activation of NLRP3 inflammasome in macrophages or diseases (34, 35). Although few studies including the one by Oh et al. revealed that MSCs can regulate the activation of NLRP3 inflammasome in macrophages or diseases (36), only one study has been reported regarding the expression of inflammasome components and their functions in MSCs (37). Moreover, in the study by Wang et al., changes in MSC function were solely focused on osteogenic and adipogenic differentiation after NLRP3 inflammasome activation. Therefore, in this study, for the first time in our knowledge, we sought to investigate whether hUCB-MSCs express NLRP3 inflammasome complexes and the activation of NLRP3 inflammasome have any influences on the immunoregulatory function of hUCB-MSCs.

Materials And Methods

Isolation and culture of hUCB-MSCs

hUCB-MSCs were provided from Kangstem Biotech (Seoul, Republic of Korea). This study was approved by Boramae Hospital Institutional Review Board (IRB. No. P01-201605-BS-02). hUCB-MSCs were cultured in complete KSB-3 complete medium (Kangstem Biotech, Seoul, Republic of Korea) with 10% fetal bovine serum (FBS; Gibco, Grand Island, NY) and 100 U/mL penicillin/streptomycin (Gibco) at 37 °C and 5% CO₂.
NLRP3 Activation In hUCB-MSCs

For NLRP3 inflammasome activation, at the confluency of 70 to 80% in relevant dishes or well plates, cells were treated with 1 µg/mL LPS (InvivoGen, San Diego, CA) for 4 hours in complete KSB-3 media. Cells were washed with phosphate-buffered saline (PBS) and 2 mM adenosine triphosphate (ATP, InvivoGen) was added followed by additional incubation for 45 minutes. Then, cells were washed again and immediately analyzed for further analysis or cultured in complete KSB media for maintenance.

RNA Extraction And PCR

The mRNA from cells was extracted with Trizol (Invitrogen, Carlsbad, CA) according to manufacturer's protocol. Then, cDNA was synthesized from 1 µg of total RNA using ReverTra Ace® qPCR RT Master Mix (Toyobo, Osaka, Japan). The PCR condition was consisted of an initial denaturation at 95 °C for 5 minutes; 35 cycles of 94 °C for 30 seconds, 60 °C for 30 seconds and 72 °C for 1 minute; a final extension at 72 °C for 5 minutes. The PCR products were separated on a 1% agarose gel, visualized, and photographed using a gel documentation system. The following primers were used: interleukin 1 receptor antagonist (IL-1RA), F: 5'-AGCTCCATCTCCACTCCAGA-3', R: 5'-GAAGAAAGAACCCCCAGGAG-3', interleukin 17 receptor A (IL-17RA), F: 5'-GGGGAGCTGTTAGCACGTAG-3', R: 5'-CAGACCCTGAAGTCACAGCA-3', interleukin 18 binding protein (IL-18BP), F: 5'-TACCTGCATTTCCACATGA-3', R: 5'-GAAGAGGCAGCATTTCAACC-3', activated leukocyte cell adhesion molecule (ALCAM), F: 5'-TAGCAGGAATGCAACTGTGG-3', R: 5'-CGCAGACATAGTTTCCAGCA-3', stromal cell-derived factor-1 alpha (SDF-1α), F: 5'-CTAGTCAAGTGCGTCCACGA-3', R: 5'-ACACACAGCCAGTCAACGAG-3'.

Protein Extraction And Western Blot Analysis

Cells were harvested and lysed using PRO-PREP Protein Extraction Solution (iNtRON Biotechnology, Seoul, Republic of Korea) according to the protocol. Samples were centrifuged at 30,000 g for 15 minutes at 4 °C and supernatants were harvested. Equivalent amounts of proteins were loaded and electrophoresed using SDS-polyacrylamide (PAGE) on 10% gel. After electrophoresis, gels were transferred to polyvinylidene difluoride (PVDF) membranes (Millipore, Billerica, MA) and membranes were blocked with blocking buffer (3% bovine serum albumin at TBST: tris-buffered saline and Tween 20) for 1 hour. Membranes were incubated with primary antibodies including NLRP3, ASC, pro/mature IL-1β, β-tubulin (Cell Signaling Technology, Danvers, MA), pro/cleaved caspase-1 (Abcam, Cambridge, MA) at 4 °C overnight. After washing with TBST buffer (10 mM Tris-Cl, 100 mM NaCl, 0.5% Tween-20), membranes

were incubated with horseradish peroxidase conjugated anti-mouse or anti-rabbit antibody (1:10000, Santa Cruz Biotechnology, CA) for 1 hour at room temperature and then washed with TBST buffer. After washing, ProNA ECL Ottimo detection kit (TransLab, Daejeon, Republic of Korea) was added at the membranes. Membranes were analyzed using ImageQuant LAS-4000 (GE Healthcare Life Sciences, Pittsburgh, PA).

Cytokine Detection And Array

Culture supernatant from naïve and NLRP3 activated-hUCB-MSCs was collected, centrifuged and stored at -80 °C. IL-1 β , IFN- γ , interleukin 4 (IL-4), interleukin 10 (IL-10), and tumor necrosis factor- α (TNF- α) concentration was measured by DuoSet ELISA kit (R&D system, Abingdon, UK) according to the protocol. PGE₂ was measured by Prostaglandin E₂ Parameter Assay Kit (R&D system). The expression level of 40 immunomodulation-related cytokines in culture supernatant was detected using C-Series Human Cytokine Array (Raybiotech, Norcross, GA).

Cell Viability And Proliferation Assay

To determine the cell viability and proliferation, Cell Counting Kit-8 (Dojindo Molecular Technologies, Rockville, MD) was used and cumulative population doubling level (CPDL) analysis was performed. For the analysis of cell death, LIVE/DEAD Viability/Cytotoxicity Kit (Invitrogen) was applied. hUCB-MSCs were seeded at 5×10^3 cells/well in 96 well plates in KSB media with 10% FBS for CCK-8 assay. After 24 hours, cells were treated with LPS/ATP/LPS + ATP and CCK-8 was added and relevant absorbance was detected according to manufacturer's instruction. For CPDL analysis, hUCB-MSCs were seeded at 6×10^4 cells/well at 6 well plate in KSB media with 10% FBS and then treated with LPS/ATP/LPS + ATP next day. Cells were subcultured every 3 day and cell numbers were counted for each subculture. The proliferation potential of early-passage and late-passage cells was determined based on the total CPDL using the formula $CPDL = \ln(N_f / N_i) / \ln 2$, where N_i and N_f are the initial and final cell count numbers, respectively, and \ln is the natural log. The population was calculated at each passage and added to the population levels of the previous passages. For LIVE/DEAD staining, cells were seeded at 8×10^4 cells/well into 12 well plates and incubated 37 °C for 24 hours. LPS and ATP were added and the cell viability of cells was measured using LIVE/DEAD cell viability assays according to the protocol.

hUCB-MSC Osteogenic Differentiation

Naïve and activated-hUCB-MSCs (ATP-MSC; LPS-MSC and LPS + ATP-MSC) were seeded in 6 well plates at a density of 1.5×10^5 cells/well in duplication at KSB-3 media. Media was changed when the confluency reaches up to 40 to 50%. Cells were cultured in the presence of specific osteogenic media containing DMEM media containing low glucose (Gibco), 10% FBS, 0.1 μ M dexamethasone and 10 mM beta-glycerophosphate (Sigma). Cells were cultured for 2 weeks and treated with LPS/ATP every 3 days and then cells were washed and media was replaced. After 2 weeks of induction, cells were fixed with 70% ethanol at 4 °C for 20 minutes after washing with PBS. Cells were washed again and stained with

1 mL of Alizarin red S (Kanto, Tokyo, Japan) at room temperature for 10 minutes. The staining solution was aspirated and then cells were washed with distilled water. To quantify the staining, 1 mL of 10% cetylpyridinium chloride (Sigma) was added to each well and incubated until complete elution of the stain at room temperature. The eluted stain was read at 570 nm using a spectrophotometer.

hUCB-MSC Adipogenic Differentiation

Naïve or stimulated-hUCB-MSCs (ATP-MSC; LPS-MSC and LPS + ATP-MSC) were seeded in 6 well plates at a density of 1.5×10^5 cells/well in duplication at KSB-3 media. Media was changed when the confluency reaches up to 80 to 90%. Cells were cultured in adipogenic differentiation media containing DMEM media containing low glucose (Gibco), 10% FBS, 0.5 mM 3-isobutyl-1-methylxanthine (Sigma) and 0.2 mM indomethacin (Sigma). Cells were cultured for 2 weeks and treated with LPS/ATP every 3 days and then cells were washed and media was replaced. After 2 weeks of differentiation, cells were fixed with 70% ethanol after washed with PBS at 4 °C for 20 minutes. Cells were washed again and stained with 1 mL of Oil Red O (Sigma) solution at room temperature for 1 hour. Staining solution was aspirated and then cells were washed with distilled water. To quantify the staining, 1 mL of 100% isopropanol (Merck, Darmstadt, German) was added to each well and incubated at room temperature. The eluted stain was read at 500 nm using a spectrophotometer.

siRNA Transfection

hUCB-MSCs were plated at the density of 2×10^5 cells/well in 6 well plate. At 50% confluency, media was changed at OPTI-MEM without penicillin/streptomycin and FBS. A mixture of transfection reagent DharmaFECT (Thermo Fisher Scientific, Waltham, MA) and ASC-siRNA (Thermo Fisher Scientific) was prepared according to the manufacturer's protocol (at a final concentration 100 nM). One day after transfection, cells were washed with PBS and harvested using TryPLE (Gibco). Harvested hUCB-MSCs were seeded again at 2×10^5 cells/well into 6 well plate with KSB media (with 10% FBS and without penicillin/streptomycin). Osteogenic differentiation was induced in naïve or ASC-inhibited hUCB-MSCs.

Flow Cytometry Analysis

The expression of positive or negative surface markers in MSCs was analyzed by flow cytometry. hUCB-MSCs were harvested and suspended in 50 µl of PBS with 5% FBS. Suspended cells were mixed with antibody solution (1:100) and incubated for 1 hour at 4 °C in the dark. Cells were stained with FITC-, PerCP/Cy5.5- or PE-conjugated antibodies specific for human CD14, CD29, CD31, CD34, CD44, CD45, CD73. Non-specific isotype-matched antibodies served as controls. After incubation, cells were washed with PBS and centrifuged for 5 minutes at 300 g. Samples were fixed with 500 µl of 0.4% paraformaldehyde/PBS. All the antibodies were purchased from BD Biosciences (Franklin Lakes, NJ) and flow cytometry analysis was performed on a FACS Caliber instruments using FlowJo software (BD).

Peripheral Blood Mononuclear Cells (PBMCs) And T Cell Proliferation

PBMC or T cell proliferation in response to Concanavalin A (ConA) or antibodies for CD3/CD28 were determined by CellTrace™ Carboxyfluorescein succinimidyl ester (CFSE) Cell Proliferation Kit (Thermo Fisher Scientific). PBMCs were prepared and labeled with CFSE according to the protocol. hUCB-MSCs were seeded at 12 well plate and NLRP3 inflammasome was activated. After NLRP3 activation, CFSE-labeled PBMCs were added to hUCB-MSCs (MSC:PBMC cell ratio, 1:10) in RPMI media 1640 (Gibco) with 10% FBS and 100 U/mL penicillin/streptomycin in the presence of 5 µg/mL concanavalin A (5 µg/mL, Sigma) or anti-CD3 (5 µg/mL, eBioscience, San Diego, CA)/anti-CD28 (2 µg/mL, eBioscience) for 5 days at 37 °C. After co-culture, cells were harvested and analyzed by flow cytometry.

Cd4+ Cell Isolation

CD4⁺ T cells were isolated from PBMCs using MACS CD4⁺ T cell isolation kit (Miltenyi Biotec, Auburn, CA). Purified T cells were cultured in RPMI 1640 with 10% FBS, 100 U/mL penicillin/streptomycin, 25 mM HEPES (Gibco), 2 mM glutamex (Gibco), 50 mM β-mercaptoethanol at 37 °C.

Th1 Differentiation

hUCB-MSCs were seeded at 12 well plate and NLRP3 inflammasome was activated. After hUCB-MSCs were activated, Th0 cells were seeded (MSC:T cell ratio, 1:10) in complete RPMI media with 10% FBS. To differentiate Th0 cells toward Th1 cells, cells were treated with anti-CD3 (5 µg/mL, eBioscience) and anti-CD28 (2 µg/mL, eBioscience), in the presence of IL-12 (10 ng/mL, Peprotech, Rocky hill, NJ) and anti-IL-4 (5 µg/mL, Peprotech) for 5 days. Media was added on day 3. After co-culture, culture supernatant was collected and IFN-γ level in supernatant was analyzed by ELISA (R&D system).

Th2 Differentiation

For Th2 cell differentiation, Th0 cells were differentiated with anti-CD3 (5 µg/mL, eBioscience) and anti-CD28 (2 µg/mL, eBioscience), in the presence of IL-4 (20 ng/mL, Peprotech) and anti-IFNγ (5 µg/mL, Peprotech) for 5 days. Media was added at day 3. After 5 days of co-culture, media was replaced with fresh media and maintained for 1 day followed by harvesting of culture. IL-4 level in conditioned media was measured by ELISA (R&D system).

Regulatory T Cell (Treg) Differentiation

Th0 cells were added to MSCs at same ratio and maintained for 5 days in complete RPMI media with 10% FBS. To prepare Treg cells as positive control group for IL-10 detection, Th0 cells were cultured with anti-CD3 (5 µg/mL, eBioscience) and anti-CD28 (2 µg/mL, eBioscience), in the presence of TGFβ (2 ng/mL, Peprotech) and IL-2 (5 µg/mL, Peprotech) for 5 days. Media was added at day 3. After co-culture, culture supernatant was collected and IL-10 level in conditioned media was detected by ELISA (R&D system).

M1 Macrophage Activation And NLRP3 Activation

THP-1 cells were obtained from Korean Cell Line Bank (Seoul, Republic of Korea). Cells were seeded at 6 well plate in RPMI media with 10% FBS and stimulated with phorbol myristate acetate (PMA, 50 ng/mL, Sigma) for 48 hours. After media replacement with normal media, THP-1 derived macrophages were stabilized for 48 hours and polarized in M1 type using LPS (10 µg/mL, invivoGen) and interferon γ (IFN-γ, 20 ng/mL, Sigma). On day 4, naïve and activated-hUCB-MSCs were added (MSC:THP-1 ratio, 1:10) in the presence of 1 µg/ml LPS (Invivogen) plus 20 ng/ml and IFN-γ (PeproTech) for the activation of macrophages. After 24 hours, culture media was harvested and TNF-α level was analyzed by ELISA (R&D system). NLRP3 activation in THP-1 derived macrophages were induced by LPS/ATP as utilized in hUCB-MSCs. THP-1 cells were seeded with naïve or pre-activated hUCB-MSCs at 6 well in RPMI media with 10% FBS (MSC:THP-1, 1:10). LPS/ATP were added and washed according to NLRP3 activation protocol. Cultured media was harvested next day and IL-1β level was measured using ELISA (R&D system).

Colitis Induction And Assessment

Male C57BL/6J mice at 8–10 weeks were obtained from Jackson Laboratory (Bar Harbor, ME). All experiments were approved by and followed the regulations of the Institute of Laboratory Animals Resources (PNUH-2016-096, Pusan National University Hospital and PNU-2018-2034 Pusan National University). Colitis was induced in mice by addition of 3%(w/v) dextran sulfate sodium (DSS; MP Biochemicals, Solon, OH) in drinking water for 7 days. 2×10^6 of hUCB-MSCs were suspended in 200 µl of PBS and injected intraperitoneally into mice 1 day after DSS administration. Mice were monitored for body weight and survival rate for 11 days and sacrificed for histopathological evaluation. Colitis severity was measured by evaluating the disease activity index including stool consistency, rectal bleeding coat roughness and general activity. The colon of DSS-treated mice was assessed for the destruction of the entire epithelium, the severity of submucosal edema, and scattered infiltration of inflammatory cells in the lamina propria and submucosa.

Statistical analysis

All results are presented as mean ± SD. All of the statistical comparisons were performed via two-tailed Student's t-test or one-way analysis of variance (ANOVA) followed by Bonferroni post hoc test for multigroup comparisons using GraphPad Prism software (version 5.01; GraphPad Software, San Diego, CA).

Results

Inflammasome components are expressed in hUCB-MSCs

We first investigated the expression of inflammasome components such as NLRP3, ASC, caspase-1, as well as final products of inflammasome activation including IL-1β in hUCB-MSCs. The expression of inflammasome components on protein level was evaluated by western blot analysis. A human monocyte leukemia cell line, THP-1 cells were used as the positive control. To activate NLRP3 inflammasome, LPS and ATP were treated for 4 hours and 45 minutes, respectively. In THP-1 cells, the expressions of NLRP3,

cleaved caspase-1 and pro/mature IL-1 β were elevated in hUCB-MSCs treated with LPS or LPS + ATP compared to the control group or ATP treated group. hUCB-MSCs expressed NLRP3, ASC, caspase-1 and IL-1 β . Interestingly, LPS + ATP treatment in hUCB-MSCs increased the expression of NLRP3, cleaved caspase-1 and pro IL-1 β . However, the expression of mature IL-1 β was not altered by LPS + ATP treatment (Fig. 1a). We next measured the production of IL-1 β and IL-18 from hUCB-MSCs after NLRP3 inflammasome activation using ELISA. However, in hUCB-MSCs, NLRP3 activation did not induce the production of IL-1 β and the basal level of IL-1 β production was too low to exert physiological functions (Fig. 1b). Moreover, the level of IL-18 production in hUCB-MSCs was not detectable (data not shown). Taken together, these findings indicate that hUCB-MSCs express the components of NLRP3 inflammasome and its activation is induced as observed in macrophages. However, the final product of its activation, mature IL-1 β , was not robustly secreted from hUCB-MSCs in response to NLRP3 activation, indicating that inflammasome activation in mesenchymal non-immune cells might serve different functions as reported in innate immune cells.

NLRP3 inflammasome stimulation does not alter the proliferation and surface marker expression of hUCB-MSCs

Pyroptosis is a caspase-1 mediated cell death which commonly occurs after inflammasome activation in macrophages and dendritic cells. Therefore, we investigated whether the viability or proliferation of hUCB-MSCs are affected by NLRP3 inflammasome activation-mediated pyroptosis. The viability and proliferation of cells were assessed by CCK-8, CPDL analysis and LIVE/DEAD staining. NLRP3 activation did not affect the viability, proliferation and death of hUCB-MSCs (Fig. 2a-c). It has been reported that stimulation of cells with ligands or cytokines can modulate the expression of surface markers in MSCs. We next analyzed the surface marker expression in naïve and activated-hUCB-MSCs. The expression pattern of all negative (CD14, CD31, CD34, CD45) or positive (CD29, CD44, CD73) markers characterizing MSCs was not altered after NLRP3 activation (Table 1, Additional file 1: Fig S1a and b). Our results imply that NLRP3 inflammasome activation in hUCB-MSCs does not induce pyroptosis nor affect the surface marker expression.

Table 1
Surface marker expression of hUCB-MSCs in response to NLRP3 inflammasome activation.

	UCB#1				UCB#2			
	(-)	LPS	ATP	LPS + ATP	(-)	LPS	ATP	LPS + ATP
CD14	0.1	0.1	0.1	0.1	0.3	0.4	0.3	0.4
CD29	100	99.9	99.9	99.9	99.8	99.9	99.4	99.9
CD31	0.4	0.6	1.2	0.7	1.1	1.4	1.3	1.0
CD34	0.2	0.1	0.1	0.1	0.3	0.4	0.3	0.5
CD44	99.9	100	100	99.9	99.8	99.7	99.0	99.9
CD45	0.5	0.5	0.4	0.6	0.2	0.3	0.3	0.3
CD73	99.7	99.8	99.8	99.7	99.8	99.7	99.2	99.9

NLRP3 Activation Inhibits The Osteogenic Differentiation Of hUCB-MSCs

Several studies have shown that differentiation of MSCs can be modulated by triggering of innate immune receptors. Therefore, the differentiation capability of hUCB-MSCs into osteoblasts or adipocytes was determined after NLRP3 inflammasome activation. The activated MSCs were cultured in specific osteogenic or adipogenic medium for two weeks and cells were stained by Alizarin red S or Oil red O, respectively. We observed that osteogenic differentiation was significantly down-regulated upon NLRP3 inflammasome activation compared with naïve hUCB-MSCs (Fig. 3a). On the other hand, NLRP3 inflammasome activation did not have any influences on the potential of adipogenic differentiation (Fig. 3b). To confirm that this inhibitory effect of NLRP3 inflammasome activation on osteogenic differentiation is mediated via inflammasome assembly, we used siRNA targeting ASC, an essential component for inflammasome assembly. ASC level was decreased after siRNA transfection in hUCB-MSCs (Fig. 3c). Interestingly, ASC suppression restored the inhibitory effect of NLRP3 inflammasome activation on osteogenic differentiation (Fig. 3d), suggesting that NLRP3 inflammasome is a negative regulator of osteogenesis in hUCB-MSCs.

NLRP3 Inflammasome Activation Augments The Immunosuppressive Properties Of hUCB-MSCs

MSCs have been reported to regulate the proliferation, activation and maturation of various immune cells. Therefore, we evaluated in vitro immunosuppressive effects of hUCB-MSCs after NLRP3 inflammasome activation. PBMCs were co-cultured with naïve or activated-MSCs at ratio of 1:10 (MSC:PBMC) with concanavalin A or anti-CD3/CD28. NLRP3 inflammasome activation enhanced the suppressive effect of hUCB-MSCs on mitogen-induced PBMC proliferation or anti-CD3/CD28-induced T cell proliferation (Fig. 4a and b). To determine whether NLRP3 inflammasome activation influences the differentiation of helper T cells, we measured Th cell type-specific cytokine production in co-culture media. Th1, Th2 and

Treg cell differentiation were assessed by detecting IFN- γ , IL-4 and IL-10 production, respectively. Both naïve or activated hUCB-MSCs significantly reduced IFN- γ production from Th1 cells (Fig. 4c). Although naïve or activated MSCs slightly inhibited IL-4 production from Th2 cells, this suppressive effect on Th2 cells was not significant. To assess the ability of MSCs to induce regulatory T cells, Th 0 cells were co-cultured with naïve or activated MSCs without any differentiation induction into Treg cells. Interestingly, IL-10 production from T lymphocytes was significantly elevated when they were co-cultured with activated MSCs (Fig. 4e).

Given that MSCs can regulate macrophage activation, we next determined the regulatory function of hUCB-MSCs on M1 activation or NLRP3 activation of macrophages using THP-1 derived macrophage-like cells. PMA-stimulated THP-1 were polarized toward M1 type TNF- α level was measured after co-culture with MSCs. When THP-1 derived macrophages were co-cultured with NLRP3 activated hUCB-MSCs, TNF- α production was downregulated to a greater extent compared to naïve MSC addition (Fig. 4f). THP-1 derived macrophages secreted increased IL-1 β in response to LPS and ATP treatment and co-culture with hUCB-MSCs suppressed IL-1 β production. Interestingly, activated hUCB-MSCs down-regulated IL-1 β production to a significantly greater extent (Fig. 4g). Taken together, these results suggest that NLRP3 inflammasome activation in hUCB-MSCs generally augments the immunoregulatory abilities including suppressive effects on T cell proliferation, Th1 cell differentiation and macrophage activation, as well as facilitating effects on Treg generation.

NLRP3 inflammasome activation improves the protective efficacy of hUCB-MSCs against DSS-induced murine colitis

Since we found that in vitro anti-inflammatory functions of hUCB-MSCs were accelerated after NLRP3 inflammasome activation, we further investigated whether this activation can lead to any beneficial effects in vivo. To this aim, DSS-induced murine colitis model was utilized because this colitic model involves T cell and macrophage-mediated immune responses in disease progression. DSS administration for one week resulted in the macroscopic symptoms of colitis, including a lethality, body weight loss, rectal bleeding, diarrhea and shortening of colon length. Intraperitoneal injection of hUCB-MSCs protected mice from lethality and body weight loss (Fig. 5a). Importantly, activated hUCB-MSCs exerted greater protective effects compared to naïve MSCs. On day 10, the disease activity index was significantly decreased by cell infusion and further improved by NLRP3 inflammasome activation (Fig. 5b). Gross findings after necropsy demonstrated that the colon length was significantly restored by the injection of hUCB-MSC from one donor (UCB#2, Fig. 5c). Upon histologic examination, destruction of the entire epithelium and scattered infiltration of inflammatory cells were observed in the colon of DSS-treated mice. In hUCB-MSC injected mice, mucosal destruction and lymphocyte infiltration were reduced (Fig. 5d). Consistent to gross evaluation, activated hUCB-MSC treatment more efficiently attenuated histopathological severity (Fig. 5d). Our findings demonstrate that NLRP3 inflammasome activation can augment the therapeutic efficacy of hUCB-MSCs in vivo, as well as in vitro anti-inflammatory abilities.

NLRP3 activation does not affect the secretion of well-known immunoregulatory soluble factors in hUCB-MSCs

MSCs have been reported to produce a variety of immunosuppressive soluble factors. To explore key soluble factors in NLRP3 inflammasome activation, we measured more than 40 soluble factors in culture media from naïve and activated hUCB-MSCs using cytokine array or ELISA. Based on the analysis of cytokine array, although there were slightly up-regulated factors including ALCAM and SDF-1 α upon NLRP3 activation in both hUCB-MSCs (Fig. 6a and Additional file 2: Fig. S2), their mRNA expression after treatment of LPS or LPS + ATP was not increased (Fig. 6b). We also investigated the expression of recently reported physiological anti-inflammatory antagonists such as IL-1RA, IL-17RA and IL-18BP. There were no significant differences between naïve and activated hUCB-MSCs in the expression of these antagonists in mRNA level (Fig. 6b). We previously suggested PGE₂ as one of the major anti-inflammatory mediators for the immunomodulatory function of MSCs. Therefore, we detected PGE₂ concentration in culture supernatant of hUCB-MSCs. However, although LPS treatment slightly increased the secretion of PGE₂, NLRP3 inflammasome activation by LPS and ATP treatment did not affect PGE₂ production (Fig. 6c). These findings propose that NLRP3 inflammasome activation potentiates the immunoregulatory functions of hUCB-MSCs presumably through the regulation of novel paracrine factors or other cell functions which have not been reported.

Discussion

Inflammasomes are multi-protein complexes that recognize inflammatory stimuli, such as PAMPs and DAMPs. The assembly of NLRP3 inflammasome complex triggers caspase-1 activation, which leads to the secretion of pro-inflammatory cytokines such as IL-1 β and IL-18, followed by pyroptosis, an inflammatory programmed cell death by the microbial pathogen (18). However, in the present study, we could not observe the pyroptosis or significant production of IL-1 β in MSC in response to NLRP3 inflammasome stimulation. Although these final phenotypes of inflammasome activation were not induced, osteogenic differentiation and immunomodulation of hUCB-MSCs were remarkably altered by NLRP3 inflammasome activation, which were not affected by single treatment of LPS or ATP. Several previous studies have shown that inflammasome or its components can regulate cell functions without classical activation of inflammasome. Wang et al. reported that NLRP3 can promote epithelial-mesenchymal transition in colon cancer cells in an inflammasome-independent manner (38). Another study by Fang et al. demonstrated that NLRP3 and ASC facilitate the expression of genes responsible for mucosal defense through the regulation of transcription factors including STAT6. In the study, authors suggested that maintenance of innate immune homeostasis by NLRP3 and ASC was inflammasome-independent (39). In addition, Kim et al. showed that hypoxia increased the expression of NLRP3 without IL-1 β production in renal tubular cells to regulate the production of mitochondrial ROS (40). Moreover, NLRP3 has been suggested as a transcriptional regulator in Th2 differentiation by binding to IL4 promoter (41).

We showed here that the osteogenic differentiation of hUCB-MSCs was impeded when NLRP3 inflammasome was activated. A number of previous researches have demonstrated that MSC differentiation can be modulated through inhibition or activation of various innate immune receptors (42). Our previous study indicated that NOD1 and NOD2 activation promoted osteogenic differentiation and decreased adipocyte differentiation (14). Moreover, TLR2 activation inhibited osteogenic, adipogenic and chondrogenic differentiation (43). Another study revealed that the activation of TLR3 and TLR4 in MSCs increased osteogenic differentiation via PI3K/AKT signaling (44). Importantly, a recent study by Wang et al. reported that human umbilical cord-derived MSCs expressed the components of NLRP3 inflammasome and that its activation inhibited osteogenic differentiation while adipogenic differentiation was enhanced (37). Consistently with this study, we observed that NLRP3 inflammasome activation suppressed the osteogenic differentiation of hUCB-MSCs, which was restored by the inhibition of ASC expression. However, adipogenesis was not enhanced in the present study and this discrepancy might be due to the difference between stimulators for inflammasome activation. We used ATP for second step activation of NLRP3 inflammasome whereas palmitic acid was used in the previous study. ATP is an established danger stimulus, which activate the purinergic $P2 \times 7$ receptor.

More importantly, in the present study, for the first time, we demonstrated that NLRP3 inflammasome activation in hUCB-MSCs led to the increased the immunosuppressive effects. Some studies reported the influence of PRR triggering on immunomodulation of MSCs. Studies from Lombardo et al. and Travassos et al. showed that TLR activation did not impair the inhibitory effect of hMSCs on the proliferation of peripheral blood mononuclear cells Lombardo, DelaRosa (13), (45). In contrast, in a study by Platten's group, TLR activation enhanced the immunosuppressive ability of hMSC by inducing IDO-1, an enzyme responsible for tryptophan catabolism (46). In addition, Waterman et al. observed that TLR4-activated hMSCs secrete pro-inflammatory mediators, while TLR3-activated hMSCs efficiently suppress inflammation Waterman, Tomchuck (47). Moreover, we previously demonstrated that NOD2 receptor stimulation with muramyl dipeptide can efficiently enhance anti-inflammatory functions of hUCB-MSCs (34, 35). In this study, NLRP3 inflammasome activation augmented the therapeutic efficacy of hUCB-MSCs in vivo, as well as in vitro anti-inflammatory abilities on several immune cells including Th cells and macrophages. This result supports the possibility that MSCs could be activated where signals for NLRP3 inflammasome activation are provided and that robust stimulation of MSCs leads to physiologically sufficient immunoregulatory effects. The limitation of our study is that crucial paracrine factors have not been discovered although we performed various screening assay upon already known major immunomodulatory factors. In this respect, it is apparent that future work will require the precise elucidation of underlying mechanism for improved function of NLRP3 inflammasome activated-MSCs by uncovering pivotal soluble factors.

Conclusion

Our findings clarified that MSCs functionally expressed NLRP3 inflammasome complex and can respond to its activation. That is, NLRP3 stimulation decreased the differentiation potential of hUCB-MSCs into osteoblasts and increased in vitro and in vivo immunosuppressive effects. We anticipate that these

findings could provide a better understanding of the inflammasome-mediated regulation of non-immune cell functions, as well as a basis for development of highly efficient cell therapy to treat several intractable inflammatory diseases.

Abbreviations

ALCAM: activated leukocyte cell adhesion molecule; ASC: apoptosis-associated speck-like protein containing a caspase recruitment domain; ATP: adenosine triphosphate; CFSE: carboxyfluorescein succinimidyl ester; Con A: Concanavalin A; CPDL: cumulative population doubling level; DSS: dextran sulfate sodium; FBS: fetal bovine serum; IDO-1: indoleamine 2,3-dioxygenase-1; IFN- γ : interferon γ ; IL-1 β : interleukin-1 β , IL-10: interleukin 10; IL-17RA: interleukin 17 receptor A; IL-18: interleukin-18; IL-18BP: interleukin 18 binding protein; IL-1RA: interleukin 1 receptor antagonist; IL-4: interleukin 4; LPS: lipopolysaccharides; MAPK: mitogen-activated protein kinase; MSC: mesenchymal stem cells; NLRP3: NLR family pyrin domain containing 3; NLRs: Nod-like receptors; NO: nitric oxide; NOD2: nucleotide-binding oligomerization domain 2; PAGE: polyacrylamide; PAMPs: pathogen-associated molecular patterns; PBMCs: Peripheral blood mononuclear cells; PBS: phosphate-buffered saline; PGE2: prostaglandin-E2; PGN: peptidoglycan; PMA: phorbol myristate acetate; PRRs: pattern recognition receptors; PVDF: polyvinylidene difluoride; SDF-1 α : stromal cell-derived factor-1 alpha; siRNA: small interfering RNA; TGF: transforming growth factor; TLRs: Toll-like receptors; TNF- α : tumor necrosis factor- α ; UCB: umbilical cord blood;

Additional Files

Additional file 1: Fig. S1. The expression of negative and positive marker for MSCs. **a**, CD14, CD31, CD34 and CD45 expression was analyzed as negative marker for MSCs. **b**, Expression of positive markers including CD29, CD44, CD73 was analyzed.

Additional file 2: Fig. S2. Cytokines in conditioned media of naïve and activated hUCB-MSCs were detected by cytokine array.

Declarations

Ethics approval and consent to participate

Not applicable

Consent for publication

Not applicable

Availability of data and material

Data and materials are available from the corresponding author on reasonable request.

Author Contributions

Conceptualization, Y.S. K.-S.K. and H.-S.K.; Methodology and data analysis, J.-S.A., Y.S., S.-J.O., J.W.Y., Y.Y.S. and B.-C.L.; Writing-original draft preparation, J.-S.A., T.-H.S.; Writing-review and editing, K.-S.K., B.-J.L. and H.-S.K.; Revision and manuscript editing, J.-S.A., E.-S.S., T.-H.S. and H.-S.K.; supervision, H.-S.K.

Funding

This research was supported by the National Research Foundation of Korea (NRF) grant funded by the Korea government (MSIT) (No. NRF-2016R1C1B2016140, NRF-2018R1A5A2023879 and NRF-2018R1D1A1B07048035).

Acknowledgments

We thank Kangstem Biotech for providing hUCB-MSCs.

Competing Interests

The authors declare no conflict of interest.

Author details

1 Department of Life Science in Dentistry, School of Dentistry, Pusan National University, Yangsan 50612, Republic of Korea

2 Dental and Life Science Institute, Pusan National University, Yangsan 50612, Republic of Korea

3 Adult Stem Cell Research Center and Research Institute for Veterinary Science, College of Veterinary Medicine, Seoul National University, Seoul 08826, Republic of Korea

4 Department of Otorhinolaryngology, Head and Neck Surgery, Pusan National University Yangsan Hospital, Yangsan, Gyeongsangnam-do 50612, Republic of Korea

5 Department of Otorhinolaryngology-Head and Neck Surgery, Biomedical Research Institute, Pusan National University School of Medicine, Pusan National University Hospital, Busan 49241, Republic of Korea

6 Translational Stem Cell Biology Branch, National Heart, Lung, and Blood Institute, National Institutes of Health, Bethesda, MD 20892, USA

References

1. Akira S, Uematsu S, Takeuchi O. Pathogen recognition and innate immunity. *Cell*. 2006;124(4):783-801.

2. Beutler B, Eidenschenk C, Crozat K, Imler JL, Takeuchi O, Hoffmann JA, et al. Genetic analysis of resistance to viral infection. *Nature reviews Immunology*. 2007;7(10):753-66.
3. Hoffmann JA. The immune response of *Drosophila*. *Nature*. 2003;426(6962):33-8.
4. Medzhitov R. Recognition of microorganisms and activation of the immune response. *Nature*. 2007;449(7164):819-26.
5. Kato H, Takahashi K, Fujita T. RIG-I-like receptors: cytoplasmic sensors for non-self RNA. *Immunol Rev*. 2011;243(1):91-8.
6. Kawai T, Akira S. Toll-like receptors and their crosstalk with other innate receptors in infection and immunity. *Immunity*. 2011;34(5):637-50.
7. Janeway CA, Jr. Approaching the asymptote? Evolution and revolution in immunology. *Cold Spring Harbor symposia on quantitative biology*. 1989;54 Pt 1:1-13.
8. Tada H, Aiba S, Shibata K, Ohteki T, Takada H. Synergistic effect of Nod1 and Nod2 agonists with toll-like receptor agonists on human dendritic cells to generate interleukin-12 and T helper type 1 cells. *Infect Immun*. 2005;73(12):7967-76.
9. Kim YG, Park JH, Shaw MH, Franchi L, Inohara N, Nunez G. The cytosolic sensors Nod1 and Nod2 are critical for bacterial recognition and host defense after exposure to Toll-like receptor ligands. *Immunity*. 2008;28(2):246-57.
10. Park JH, Kim YG, Shaw M, Kanneganti TD, Fujimoto Y, Fukase K, et al. Nod1/RICK and TLR signaling regulate chemokine and antimicrobial innate immune responses in mesothelial cells. *J Immunol*. 2007;179(1):514-21.
11. van den Berk LC, Jansen BJ, Siebers-Vermeulen KG, Netea MG, Latuhihin T, Bergevoet S, et al. Toll-like receptor triggering in cord blood mesenchymal stem cells. *J Cell Mol Med*. 2009.
12. Tomchuck SL, Zwezdaryk KJ, Coffelt SB, Waterman RS, Danka ES, Scandurro AB. Toll-like receptors on human mesenchymal stem cells drive their migration and immunomodulating responses. *Stem Cells*. 2008;26(1):99-107.
13. Lombardo E, DelaRosa O, Mancheno-Corvo P, Menta R, Ramirez C, Buscher D. Toll-like receptor-mediated signaling in human adipose-derived stem cells: implications for immunogenicity and immunosuppressive potential. *Tissue Eng Part A*. 2009;15(7):1579-89.
14. Kim H-S, Shin T-H, Yang S-R, Seo M-S, Kim D-J, Kang S-K, et al. Implication of NOD1 and NOD2 for the differentiation of multipotent mesenchymal stem cells derived from human umbilical cord blood. *PLoS One*. 2010;5(10):e15369.

15. Hwa Cho H, Bae YC, Jung JS. Role of toll-like receptors on human adipose-derived stromal cells. *Stem Cells*. 2006;24(12):2744-52.
16. Vajjhala PR, Mirams RE, Hill JM. Multiple binding sites on the pyrin domain of ASC protein allow self-association and interaction with NLRP3 protein. *Journal of Biological Chemistry*. 2012;287(50):41732-43.
17. Martina P, Motti G, Peter DM, John CR, Stefan JR. The CARD plays a critical role in ASC foci formation and inflammasome signalling. *Biochemical Journal*. 2013;449(3):613-21.
18. Broderick L, De Nardo D, Franklin BS, Hoffman HM, Latz E. The inflammasomes and autoinflammatory syndromes. *Annual Review of Pathology: Mechanisms of Disease*. 2015;10:395-424.
19. Bauernfeind FG, Horvath G, Stutz A, Alnemri ES, MacDonald K, Speert D, et al. Cutting edge: NF- κ B activating pattern recognition and cytokine receptors license NLRP3 inflammasome activation by regulating NLRP3 expression. *The Journal of Immunology*. 2009;183(2):787-91.
20. Yu J, Nagasu H, Murakami T, Hoang H, Broderick L, Hoffman HM, et al. Inflammasome activation leads to Caspase-1-dependent mitochondrial damage and block of mitophagy. *Proceedings of the National Academy of Sciences*. 2014;111(43):15514-9.
21. Augello A, Tasso R, Negrini SM, Cancedda R, Pennesi G. Cell therapy using allogeneic bone marrow mesenchymal stem cells prevents tissue damage in collagen induced arthritis. *Arthritis & Rheumatism*. 2007;56(4):1175-86.
22. Gonzalez MA, Gonzalez-Rey E, Rico L, Buscher D, Delgado M. Adipose-derived mesenchymal stem cells alleviate experimental colitis by inhibiting inflammatory and autoimmune responses. *Gastroenterology*. 2009;136(3):978-89.
23. Le Blanc K, Rasmusson I, Sundberg B, Gotherstrom C, Hassan M, Uzunel M, et al. Treatment of severe acute graft-versus-host disease with third party haploidentical mesenchymal stem cells. *The Lancet*. 2004;363(9419):1439-41.
24. Lee RH, Seo MJ, Reger RL, Spees JL, Pulin AA, Olson SD, et al. Multipotent stromal cells from human marrow home to and promote repair of pancreatic islets and renal glomeruli in diabetic NOD/scid mice. *Proceedings of the National Academy of Sciences*. 2006;103(46):17438.
25. Nemeth K, Leelahavanichkul A, Yuen PST, Mayer B, Parmelee A, Doi K, et al. Bone marrow stromal cells attenuate sepsis via prostaglandin E2-dependent reprogramming of host macrophages to increase their interleukin-10 production. *Nature medicine*. 2008;15(1):42-9.
26. Zappia E, Casazza S, Pedemonte E, Benvenuto F, Bonanni I, Gerdoni E, et al. Mesenchymal stem cells ameliorate experimental autoimmune encephalomyelitis inducing T-cell anergy. *Blood*. 2005;106(5):1755.

27. Ren G, Zhang L, Zhao X, Xu G, Zhang Y, Roberts AI, et al. Mesenchymal stem cell-mediated immunosuppression occurs via concerted action of chemokines and nitric oxide. *Cell stem cell*. 2008;2(2):141-50.
28. Krampera M, Glennie S, Dyson J, Scott D, Laylor R, Simpson E, et al. Bone marrow mesenchymal stem cells inhibit the response of naive and memory antigen-specific T cells to their cognate peptide. *Blood*. 2003;101(9):3722.
29. Beyth S, Borovsky Z, Mevorach D, Liebergall M, Gazit Z, Aslan H, et al. Human mesenchymal stem cells alter antigen-presenting cell maturation and induce T-cell unresponsiveness. *Blood*. 2005;105(5):2214.
30. Puissant B, Barreau C, Bourin P, Clavel C, Corre J, Bousquet C, et al. Immunomodulatory effect of human adipose tissue derived adult stem cells: comparison with bone marrow mesenchymal stem cells. *British journal of haematology*. 2005;129(1):118-29.
31. Yanez R, Lamana ML, Garcia Castro J, Colmenero I, Ramirez M, Bueren JA. Adipose Tissue Derived Mesenchymal Stem Cells Have In Vivo Immunosuppressive Properties Applicable for the Control of the Graft Versus Host Disease. *Stem cells*. 2006;24(11):2582-91.
32. Sato K, Ozaki K, Oh I, Meguro A, Hatanaka K, Nagai T, et al. Nitric oxide plays a critical role in suppression of T-cell proliferation by mesenchymal stem cells. *Blood*. 2007;109(1):228.
33. Tse WT, Pendleton JD, Beyer WM, Egalka MC, Guinan EC. Suppression of allogeneic T-cell proliferation by human marrow stromal cells: implications in transplantation. *Transplantation*. 2003;75(3):389.
34. Kim HS, Shin TH, Lee BC, Yu KR, Seo Y, Lee S, et al. Human umbilical cord blood mesenchymal stem cells reduce colitis in mice by activating NOD2 signaling to COX2. *Gastroenterology*. 2013;145(6):1392-403 e1-8.
35. Kim HS, Yun JW, Shin TH, Lee SH, Lee BC, Yu KR, et al. Human umbilical cord blood mesenchymal stem cell-derived PGE₂ and TGF-beta1 alleviate atopic dermatitis by reducing mast cell degranulation. *Stem Cells*. 2015;33(4):1254-66.
36. Oh JY, Ko JH, Lee HJ, Yu JM, Choi H, Kim MK, et al. Mesenchymal stem/stromal cells inhibit the NLRP3 inflammasome by decreasing mitochondrial reactive oxygen species. *Stem Cells*. 2014;32(6):1553-63.
37. Wang L, Chen K, Wan X, Wang F, Guo Z, Mo Z. NLRP3 inflammasome activation in mesenchymal stem cells inhibits osteogenic differentiation and enhances adipogenic differentiation. *Biochem Biophys Res Commun*. 2017;484(4):871-7.

38. Wang H, Wang Y, Du Q, Lu P, Fan H, Lu J, et al. Inflammasome-independent NLRP3 is required for epithelial-mesenchymal transition in colon cancer cells. *Exp Cell Res*. 2016;342(2):184-92.
39. Fang R, Uchiyama R, Sakai S, Hara H, Tsutsui H, Suda T, et al. ASC and NLRP3 maintain innate immune homeostasis in the airway through an inflammasome-independent mechanism. *Mucosal Immunol*. 2019;12(5):1092-103.
40. Kim SM, Kim YG, Kim DJ, Park SH, Jeong KH, Lee YH, et al. Inflammasome-Independent Role of NLRP3 Mediates Mitochondrial Regulation in Renal Injury. *Front Immunol*. 2018;9:2563.
41. Bruchard M, Rebe C, Derangere V, Togbe D, Ryffel B, Boidot R, et al. The receptor NLRP3 is a transcriptional regulator of TH2 differentiation. *Nat Immunol*. 2015;16(8):859-70.
42. DelaRosa O, Dalemans W, Lombardo E. Toll-like receptors as modulators of mesenchymal stem cells. *Frontiers in immunology*. 2012;3.
43. Pevsner-Fischer M, Morad V, Cohen-Sfady M, Rousso-Noori L, Zanin-Zhorov A, Cohen S, et al. Toll-like receptors and their ligands control mesenchymal stem cell functions. *Blood*. 2007;109(4):1422-32.
44. Wang Zj, Zhang Fm, Wang Ls, Yao Yw, Zhao Q, Gao X. Lipopolysaccharides can protect mesenchymal stem cells (MSCs) from oxidative stress-induced apoptosis and enhance proliferation of MSCs via Toll-like receptor (TLR)-4 and PI3K/Akt. *Cell biology international*. 2009;33(6):665-74.
45. Travassos LH, Girardin SE, Philpott DJ, Blanot D, Nahori MA, Werts C, et al. Toll-like receptor 2-dependent bacterial sensing does not occur via peptidoglycan recognition. *EMBO Rep*. 2004;5(10):1000-6.
46. Opitz CA, Litzemberger UM, Lutz C, Lanz TV, Tritschler I, Koppel A, et al. Toll-like receptor engagement enhances the immunosuppressive properties of human bone marrow-derived mesenchymal stem cells by inducing indoleamine-2,3-dioxygenase-1 via interferon-beta and protein kinase R. *Stem cells*. 2009;27(4):909-19.
47. Waterman RS, Tomchuck SL, Henkle SL, Betancourt AM. A new mesenchymal stem cell (MSC) paradigm: polarization into a pro-inflammatory MSC1 or an immunosuppressive MSC2 phenotype. *PLoS One*. 2010;5(4):e10088.

Figures

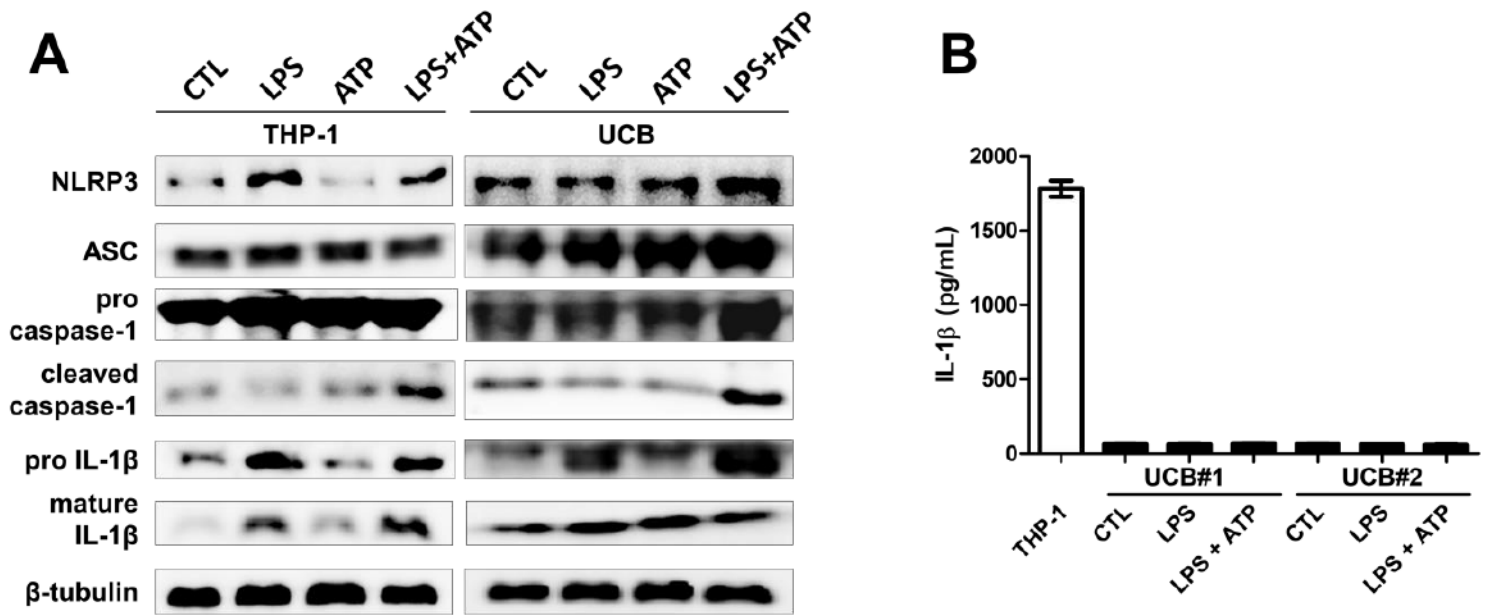


Figure 1

The expression of inflammasome components and products in hUCB-MSCs. a, Expressions of NLRP3, ASC, pro or cleaved caspase-1, pro or mature IL-1 β were analyzed by immunoblotting in hUCB-MSCs after treatment with LPS, ATP or LPS+ATP. THP-1 cells were used as a control group. b, Concentration of mature IL-1 β in culture supernatant of hUCB-MSCs was measured by ELISA. Results are shown as mean \pm SD.

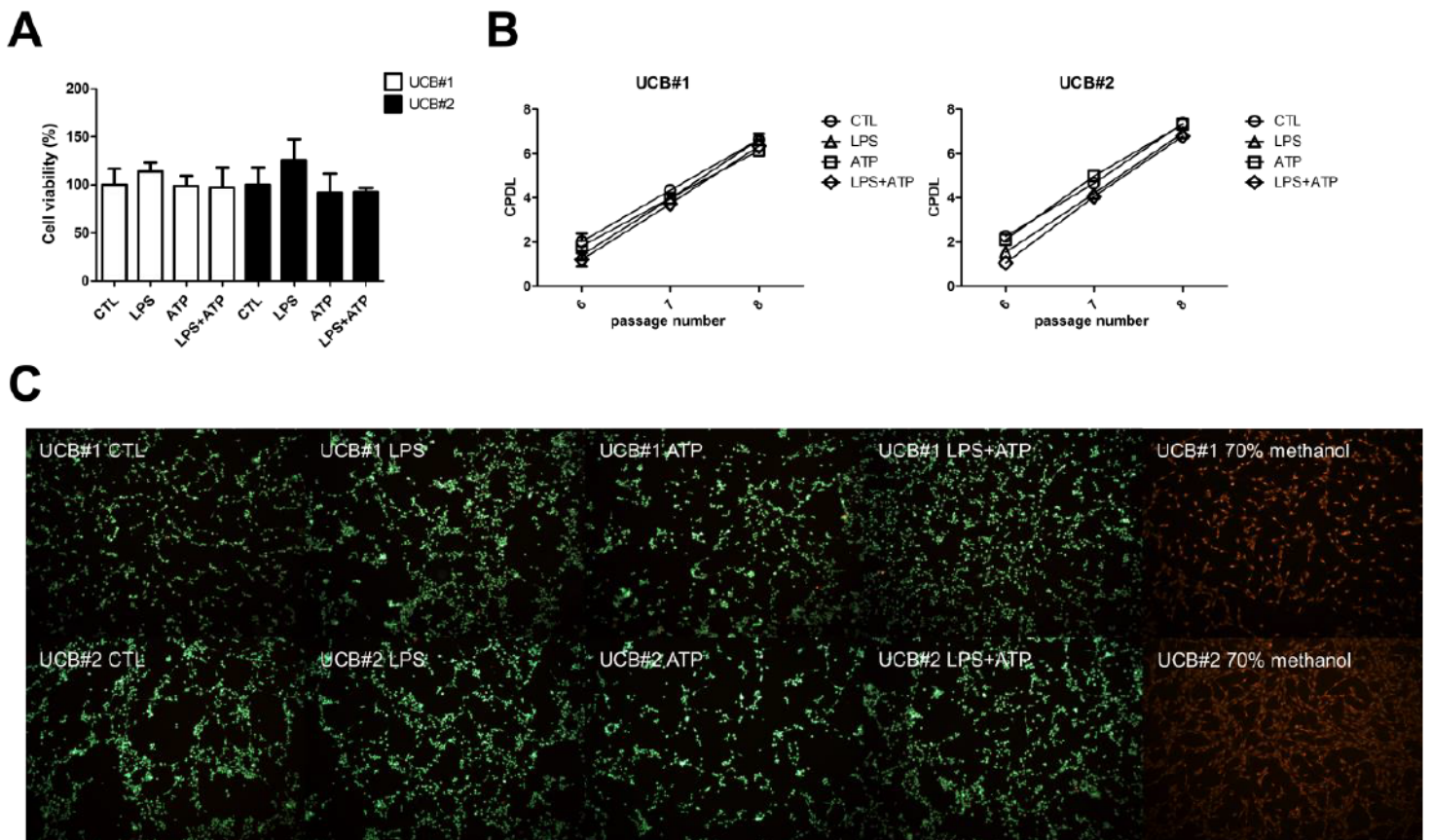


Figure 2

Viability, proliferation and death of hUCB-MSCs after NLRP3 inflammasome activation. a-c, hUCB-MSCs were stimulated with LPS, ATP or LPS+ATP followed by the determination for cell viability, proliferation and death. a, Cell viability was detected by CCK-8. b, Cell proliferation was determined by CPDL analysis. c, Cell death was assessed by Live/Dead staining. 70% methanol was treated to induce cell death in hUCB-MSCs as a control group. Bar, 500 μ m. Results are shown as mean \pm SD.

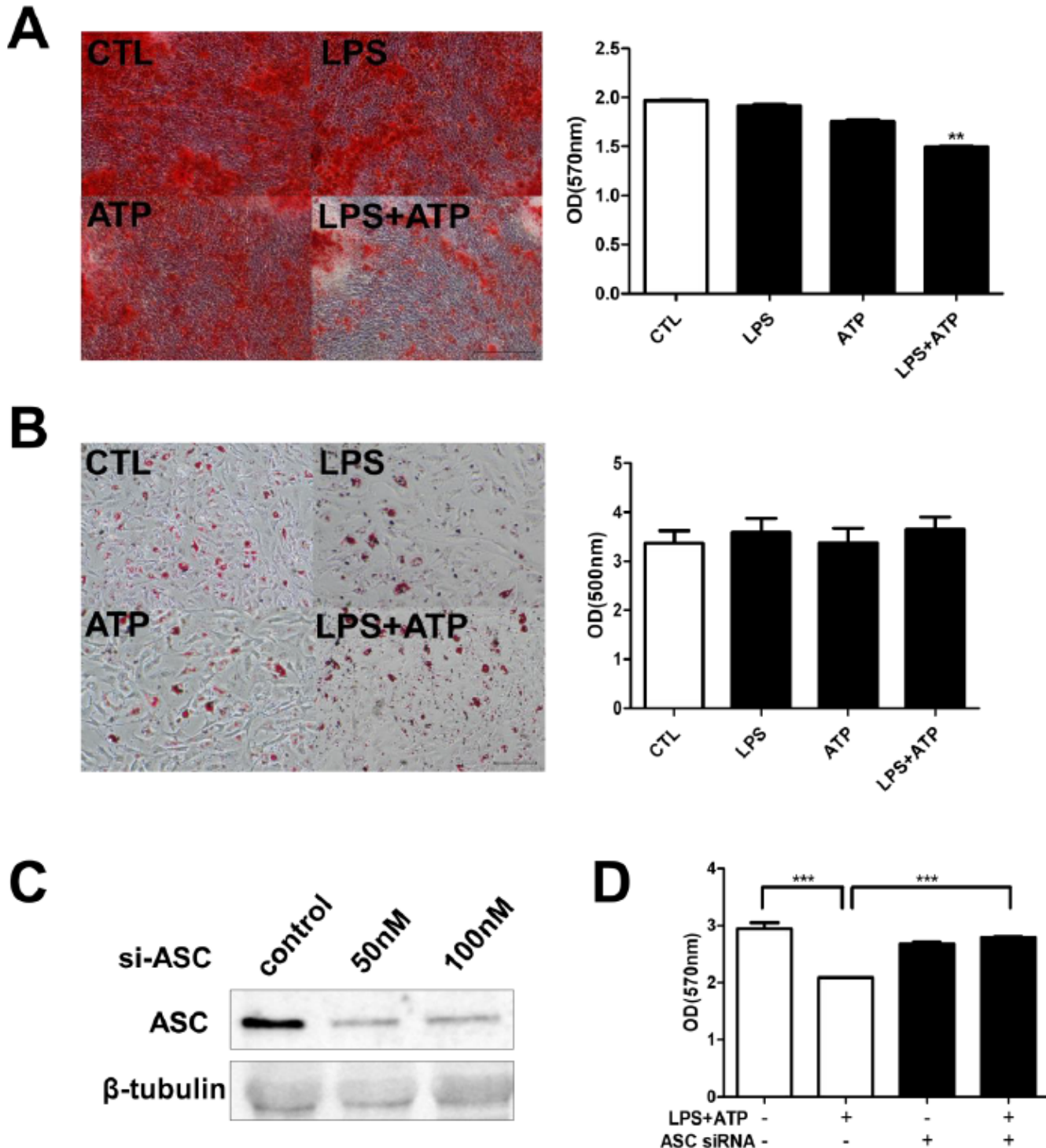


Figure 3

Osteogenic and adipogenic differentiation of NLRP3-activated hUCB-MSCs. a, hUCB-MSCs were cultured in induction media for osteoblast differentiation in the presence or absence of stimulants for NLRP3 inflammasome activation. Osteoblasts were stained with Alizarin Red S and quantified. Stain was eluted by acetylpyridinium chloride and the absorbance was measured at 570 nm. Bar, 25 μ m. b, Naïve or NLRP3-activated hUCB-MSCs were differentiated into adipocytes using conditioned media and the accumulation of lipid droplets in the cytosol was determined by Oil Red O staining. Stain was eluted by 100% isopropanol and the absorbance was measured at 500 nm. Bar, 500 μ m. c, siRNA for ASC was transfected to hUCB-MSCs and decrease in ASC expression on protein level was determined by western blot. d, siRNA-treated hUCB-MSCs were harvested and seeded for osteogenic differentiation. Eluted stain for osteoblasts was quantified by measuring absorbance. Results are shown as mean \pm SD. **P < .01, ***P < .001.

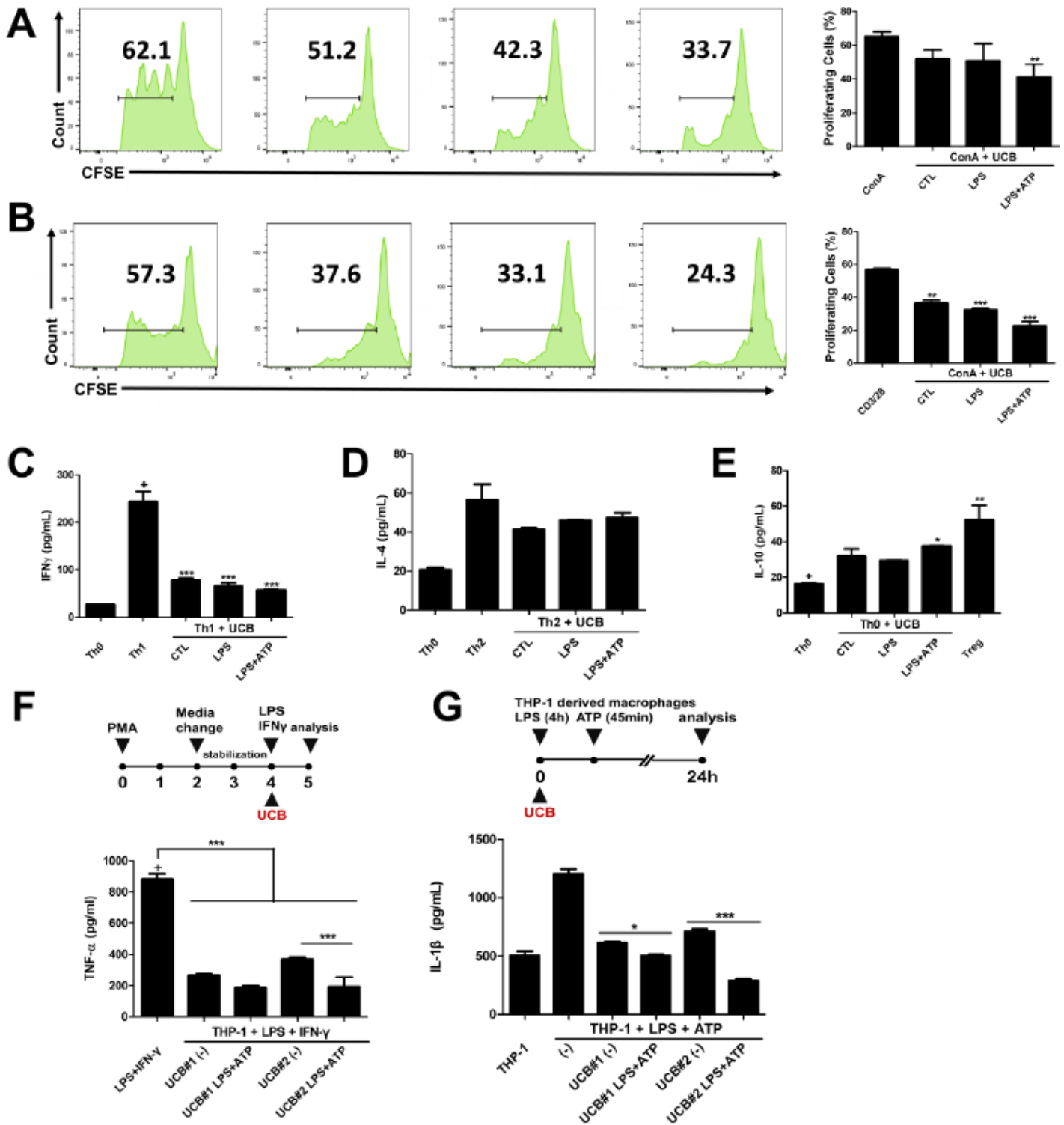


Figure 4

Immunoregulatory properties of NLRP3-stimulated hUCB-MSCs. a and b, PBMCs were stained with CFSE and then activated by concanavalin A (a) or anti-CD3/28 (b), to induce the proliferation of pan lymphocytes or T cells, respectively. PBMCs were co-cultured with naïve or activated hUCB-MSCs and cell proliferation was analyzed by measuring CFSE intensity using flow cytometry. c-e, CD4⁺ T cells isolated from PBMCs were co-cultured with hUCB-MSCs. c and d, Th1 and Th2 cell differentiation was induced in

the presence or absence of hUCB-MSCs. IFN- γ and IL-4 productions were measured using ELISA. e, Naive CD4⁺ T cells were co-cultured with hUCB-MSCs and IL-10 production was measured to determine the induction of Treg differentiation. f, THP-1 derived macrophages were activated for M1 polarization and co-cultured with hUCB-MSCs. TNF- α in cultured media was detected by ELISA. g, NLRP3-activated THP-1 derived macrophages were co-cultured with hUCB-MSCs. IL-1 β in culture media was detected by ELISA. Results are shown as mean \pm SD. *P < .05, **P < .01, ***P < .001.

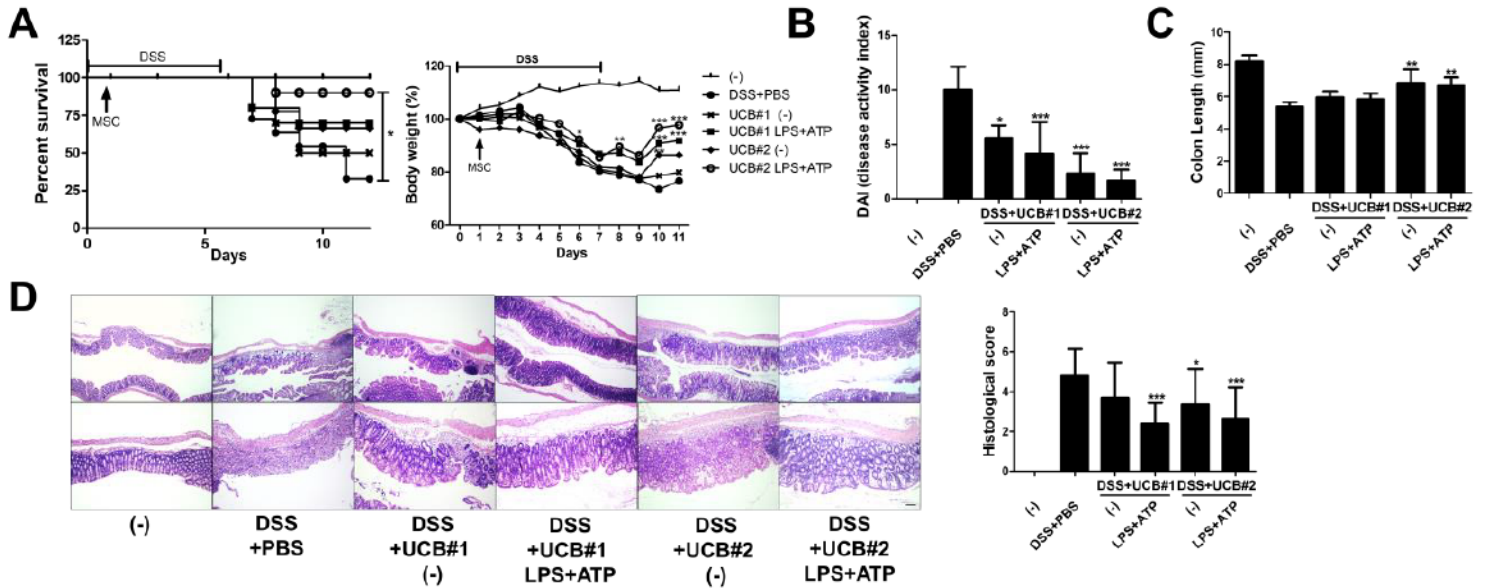


Figure 5

Therapeutic efficacy of NLRP3-stimulated hUCB-MSCs in DSS-induced colitis model. a-d, DSS-induced colitis mice were i.p. injected with naïve and activated hUCB-MSCs, followed by monitoring for gross and histological evaluation. (-) denotes control group provided with normal drinking water. Numbers of mice per group; (-), 6; DSS+PBS, 11; DSS+UCB#1 (-), 10; DSS+UCB#1 LPS+ATP, 10; DSS+UCB#2 (-), 9; DSS+UCB#2 LPS+ATP, 10. a, Mice were monitored for survival rate and body weight loss. b, At day 10, disease activity index was determined. c, After sacrifice on day 12, colon length was measured. d, Colon sections were prepared and stained with H&E. Histopathologic evaluation was performed by determining the destruction of epithelial structure and lymphocyte infiltration. Upper panels: 40X, lower panels: 100X, bar, 500 μ m. Results are shown as mean \pm SD. *P < .05, **P < .01, ***P < .001.

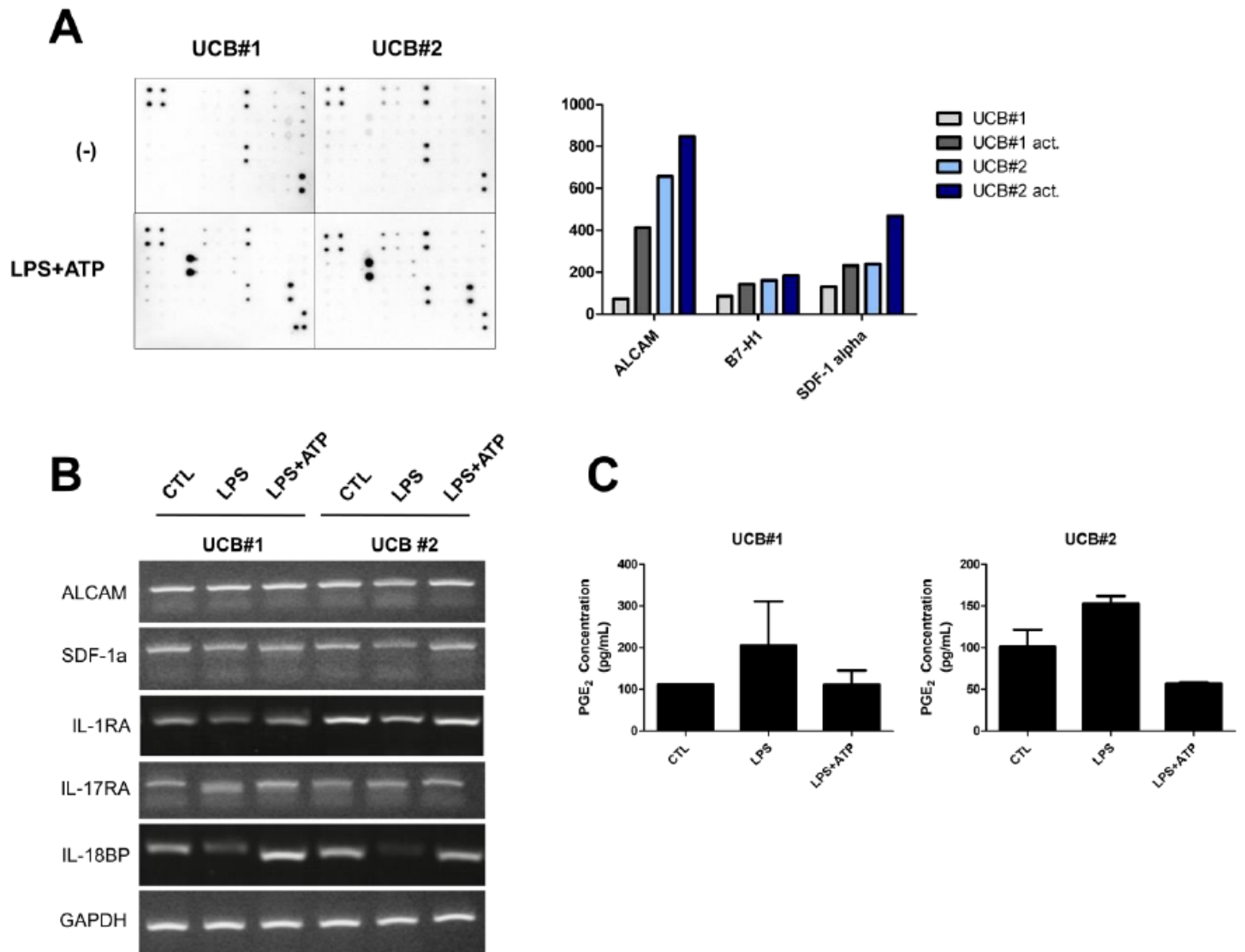


Figure 6

Screening for immunoregulatory soluble factors in NLRP3-activated hUCB-MSCs. a, Cytokines in conditioned media of naïve or activated hUCB-MSCs were analyzed by cytokine array. Commonly up-regulated factors in both hUCB-MSCs were presented. b, mRNA expression level of ALCAM, SDF-1 α , IL-1RA, IL-17RA and IL-18BP in hUCB-MSCs were analyzed by PCR. c, PGE₂ concentration in culture supernatant of hUCB-MSCs was measured by ELISA. Results are shown as mean \pm SD

Supplementary Files

This is a list of supplementary files associated with this preprint. Click to download.

- [Additionalfile2.docx](#)
- [Additionalfile1.docx](#)